Seoul inter-noise 2020 23 - 26 AUGUST

Sound leakage investigation of ANC headphones using particle velocity sensors

Fanyu Meng[1]
Microflown Technologies
Tivolilaan 205, 6824 BV Arnhem, The Netherlands

Anbo Yu[2]
HT Acoustics
B - 707, R&D Plaza, Shuangqing Road, Haidian District, Beijing, China

Dani Fernandez[3]
Microflown Technologies
Tivolilaan 205, 6824 BV Arnhem, The Netherlands

ABSTRACT

Active noise control (ANC) headphones have received wide attention globally in recent years. Apart from developing more advanced noise cancellation algorithms, another challenge the ANC headphone industry faces is the selection of microphone positioning, which would significantly influence the performance of active noise cancellation. The materials and structures of the headphone cups lead to inhomogeneous distribution of sound leakage. When the microphone is placed on positions with different leakage, it sends different feedback to the ANC system and results in different performance. Therefore, the positioning of the microphone plays a critical role in the noise cancellation effect. The particle velocity sensor can significant restrict background noise due to its high directivity, and thus suitable to apply for in-situ sound localization. This work applies the particle velocity sensor to thoroughly scan around the ANC headphones and localize the main leaking spots. The microphone is then placed in the detected spots, and the noise cancellation performance is compared.

1. INTRODUCTION

Active noise control (ANC, or active noise cancellation) headphones have been receiving increasing attention by the public during the past years. By definition, the ANC system generates an anti-noise to cancel the unwanted noise propagating to the ear [1]. As headphones are exposed to various, time-varying environments with unknown sources, a microphone to capture ambient sounds is normally necessary. This sensor is called reference microphone, which measures and feeds a reference signal to the ANC system. With the loudspeaker of the headphone generating anti-noise, an error microphone inside the earcup is used to record the in-ear sound to monitor the performance

[1]meng@microflown.com

[2]yuanbo@ht-acoustics.com

[3]fernandez@microflown.com

of ANC [2]. The acoustic transfer function between the reference and error microphones is called primary path, and the secondary path describes the transfer path between the headphone speaker to the error microphone [3]. In terms of the acoustic path, the feedforward ANC relies on both of them, whereas feedback ANC is only dependent on the secondary path.

The performance of ANC highly depends on signal processing algorithms and the physical system. They still remain challenges nowadays, despite the rapid development of many noise cancelling approaches during the last decade [2]. In general, the ANC system can be summarized in feedforward, feedback and hybrid systems depending on the algorithms being used. Besides the implemented methodology, the physical essence of the system is also of critical importance to the overall ANC performance. The mechanical design of an ANC headphone should consider the factors that influence the acoustical performance, such as noise sources in the surrounding environment, the positioning of transducers and the vibro-acoustic performance of the device [2].

The direction-of-arrival (DOA) of the ambient sound sources can lead to large deviations on the acoustic performance at high frequencies. The DOA causes deviations in the primary path and thus could deteriorate the performance of feedforward ANC [3]. Also for feedforward ANC, Iwai et al. proposed to utilize a reference microphone array to separate noise sources and aim at the main source to effectively reduce the disturbance noise [4]. The authors stated that the locations of the reference microphones determine the noise reduction ability of multichannel ANC systems. However, the positioning of the reference microphone was not further investigated. For the error microphone, an optimized position was determined and evaluated by comparing the flatness of the frequency responses of secondary paths with the error microphone in various locations [5]. Eight locations were studied, and it was discovered that the frequency responses can largely deviate, in some frequency ranges even up to 40 dB.

Altering the structure of the headphone can influence the sound fields inside and outside of the headphone earcup, and thus can change the acoustic paths, resulting in the deterioration of the ANC performance. This includes sound leakage mainly from the gap between the earcup cushion and pinna, due to either the way of wearing the headphone [6], or the conjunction parts of the earcup. Additionally, resonances on the earcup could also lead to undesired acoustic paths. The leakage and resonance can decrease the correlation between the signals captured by the reference and error microphones and increases residual noise. A hybrid method was proposed to tackle this problem with the improvement of noise reduction and fast convergence speed [7]. Leakage could lead to a decrease at low frequencies in the magnitude response and delay of the secondary path [8], which can deteriorate both feedforward and feedback ANC systems [9]. A Leaky-FXLMS algorithm was proposed to overcome the limitations of the FXLMS algorithm, such as ill-conditioned input signal and the nonlinearities of the system components, which can be caused by leakage [10]. However, before stepping into the signal processing stage, it is necessary to start with the physical nature of the structure, to analyse the sound field, and localize the leakage and resonance. This can help not only to improve the structure, but also to position the microphones. As a result, it is possible to enhance the ANC performance in this physical way without increasing the complexity of the algorithms.

Conventional sound pressure-based techniques for detecting the leakage often encounter difficulties assessing small devices, such as headphones, especially in non-anechoic environments. The high levels of background noise and reverberation, along with the low excitation emitted by the device under assessment, prevent the acquisition of acoustic data in-situ [11]. In contrast, the use of acoustic particle velocity transducers offers a significant advantage over conventional testing techniques. The vector nature of particle velocity, an intrinsic dependency upon surface displacement and sensor directivity are the main advantages over conventional solutions. As a result, quantitative measurements describing the vibro-acoustic behaviour of a device or structure can be performed in a regular environment [12]. The particle velocity sensor was successfully used to detect acoustic leakage inside a car [13]. To have a better understanding about the sound field and leakage around the headphone, sound visual representations can play a key role [14]. A 3D visualization of vectorial

fields can be achieved based on the "Scan & Paint" technique with a 3D intensity probe [15]. The 3D intensity probe is manually moved whilst a stereo camera is used to extract the instantaneous spatial position of the intensity probe. The recorded signals are split into multiple segments and assigned to a set of positions using a spatial discretization algorithm. A vector representation of the acoustic variations across the sound field can then be computed combining the sound pressure and the three orthogonal acoustic particle velocities. Results are presented over a 3D sketch of the tested object, obtaining a visual representation of the sound distribution around the object [14]. Hence, the sound field around the headphone can be demonstrated in full 3D, and potential leakage spots and resonances can be visualized.

This work focuses on analyzing the sound field of ANC headphones to detect potential leakages and resonances by means of fast in-situ detection and full 3D sound field visualization using particle velocity sensors. The measurement results and main findings will be presented in the following sections.

2. POSITIONING OF THE REFERENCE MICROPHONE

A preliminary study was conducted to have an initial understanding about how positioning the reference microphone affects the ANC performance. Three points on the external surface of the earcup were selected, i.e. A, B and O as shown in Figure 1. Two measurements were performed with two configurations: reference microphones positioned at point A and O (PA and PO, Figure 1(a), to evaluate the ANC performance. The measurement "point" will be simplified as "P" throughout the paper.), and at PB and PO (Figure 1(b)).

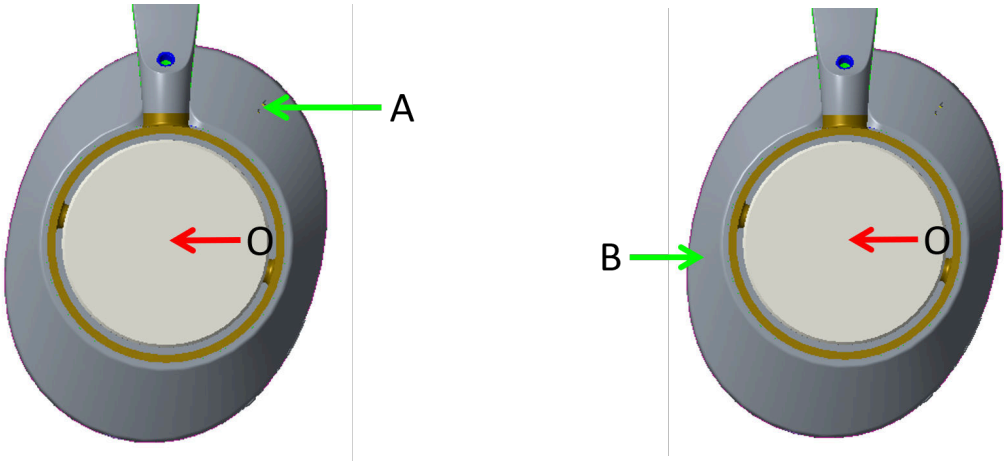

(a) Reference microphones at PA and PO *(b) Reference microphones at PB and PO*

Figure 1: Two configurations of reference microphone positions

Since the position of the reference microphone is the variable for this study, only feedforward algorithm is evaluated. The feedforward algorithm can be denoted as [3]:

$$\frac{E(z)}{X(z)} = P(z) - G(z)W(z), \tag{1}$$

where $X(z)$ and $E(z)$ are the z-transform of the signal $x(t)$ and $e(t)$ measured at the reference and error microphones, $P(z)$ and $G(z)$ represent the primary and secondary paths, and $W(z)$ is the control filter.

Figure 2 shows the noise reduction with the two configurations. Due to measurement uncertainties and algorithm dispersion, the performance of PO is not totally consistent between the two measurements. It can be seen that positioning the reference microphone at PO outperforms PA or PB. The noise reduction difference can reach 10 dB in Figure 2(a) at some frequencies.

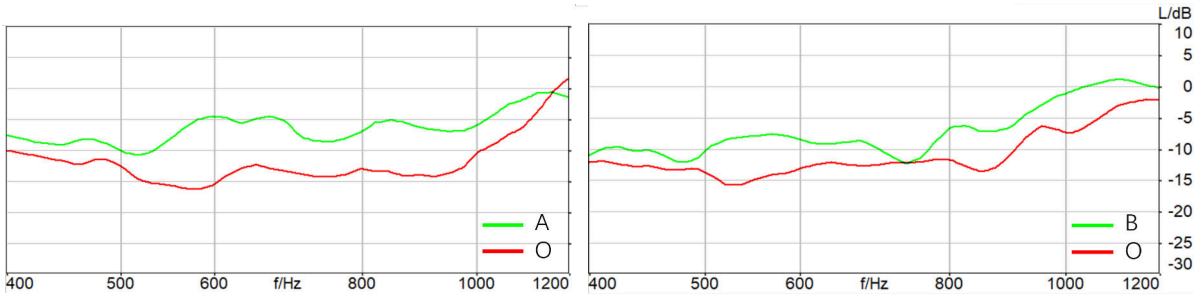

(a) PA vs. PO *(b) PB vs. PO*

Figure 2: ANC performance (Noise reduction) with the reference microphone at different positions

The reference microphones at various positions on the earcup captured different sounds and feed in the feedforwrad ANC system, which leads to the variations in the noise reduction performance. Recalling the error microphone positioning study in [5], it reveals the importance of examining the sound field around the earcup which can be quite critical for positioning both the reference and error microphones. Another possible reason that needs to be mentioned is that the correlation between the reference and error microphones could be higher when the reference microphone is at PO, which results in better performance at this point.

3. FAST IN-SITU DETECTION WITH VOYAGER

This works employs the acoustic reciprocity to study the sound leakage on the headphone earcup. White noise was played by the loudspeaker in the earcup on one side of the device, and the acoustic sensors were placed outside of the earcup to measure the sound field. This method facilitates to understand how the sound is leaked from the sensor positions to the loudspeaker.

A handheld vibroacoustic device called Voyager is first used to conduct fast leakage detection. The Voyager contains a PU probe, which comprises a microphone and a particle velocity sensor [16]. Five ANC headphones were tested using Voyager. The PU probe was set 5 mm away from the earcup surface (two of the measurement setups are visible in Figure 3).

The experiments were conducted with five headphones of four different brands, with HP2A and HP2B being two different sets of the same model, same brand. Figure 4 shows the measured particle velocity level (PVL) and sound pressure level (SPL) at the reference microphone positions of the five headphones. Large variations exist between headphones, even between HP2A and HP2B. In general, PVL in Figure 4(a) shows a larger dynamic range than SPL in Figure 4(b). This is due to the directivity of the particle velocity sensor, along with the intrinsic dependency on surface displacement perceived in the near field, enabling an accurate localization of the leakage. Therefore, high PVL (72 dB) can be observed when HP1's reference microphone is at 600 Hz, and the PVL of HP4 is below 30 dB in the range of 600 - 1000 Hz. While for SPL, there is only about 15 dB difference between HP1 and HP4, which is much less than the 40 dB of PVL at around 600 Hz.

The particle velocity spectra of different components of HP2B on the earcup are plotted in Figure 5. The leakage mainly lies in the range of 300 - 1600 Hz, which is within the target frequency range of ANC. Although from the same device, large variations are apparent when the probe is positioned in front of different mechanical components, even comparable to those in Figure 4. It is thus necessary to explore in-depth how the emitted sound is distributed around the earcup.

The earcup of HP2B is then discretized into 17 points for further analysis (Figure 6). We name the surface on the earcup which P9-P17 are pointing to as the side of the earcup, and the surface containing P1-P8 as the ring of the earcup. Figure 3 demonstrates two measurements on the side and ring of the earcup, respectively.

For the sake of clarity, only results of key points are illustrated in Figure 7. Two frequency ranges

(a) PU probe pointing to the side of the earcup *(b) PU probe pointing to the ring of the earcup*

Figure 3: Headphone measurement setup with Voyager

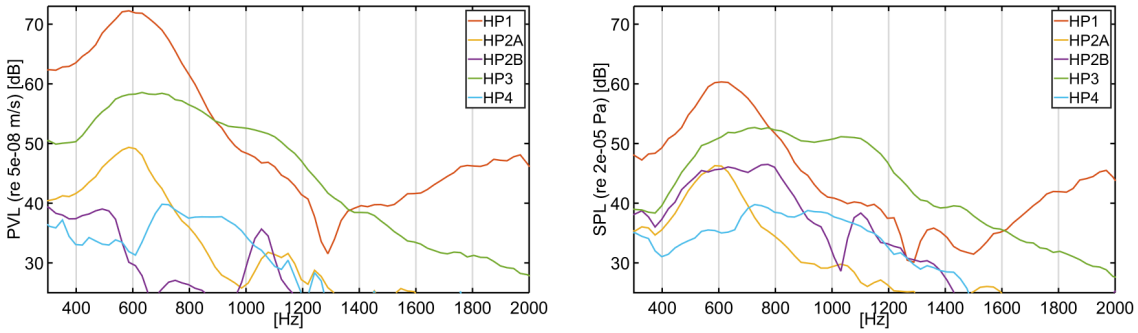

(a) Particle velocity level *(b) Sound pressure level*

Figure 4: Spectra of measurements on the reference microphones of five different ANC headphones

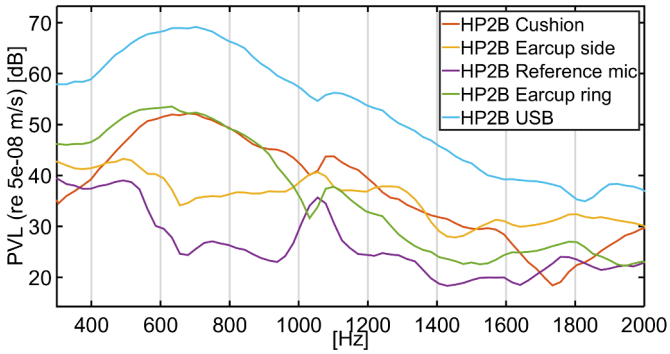

Figure 5: Particle velocity spectra of different components of HP2B

are of interest, 600 - 1000 Hz and 1000 - 1200 Hz since there are peaks which can indicate leakages in these two ranges. In 600 - 1000 Hz, P10, P11 and P13 show peaks and dips, whereas P9 and P12 only show dips, as in Figure 7(a). The side of the earcup seems to have a natural resonance within

this frequency range. Another peak between 1000 Hz and 1200 Hz can be observed for all the points. For SPL in Figure 7(b), there is no significant difference between the spectra as they show similar trend. The broadband directivity of the particle velocity sensor assures the reduction of noise from other directions, and only the part of the surface that the sensor pointing to is measured. As the sensor is quite close to the surface, the measured particle velocity is related to the surface velocity [17]. Therefore, the particle velocity can detect potential modal behaviour with high spatial resolution in the near field, which is in line with [12].

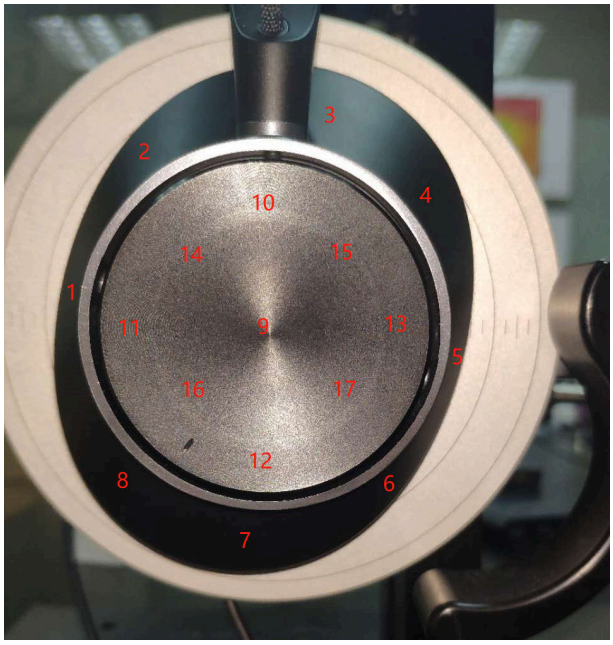

Figure 6: Discretized measurement points of HP2B

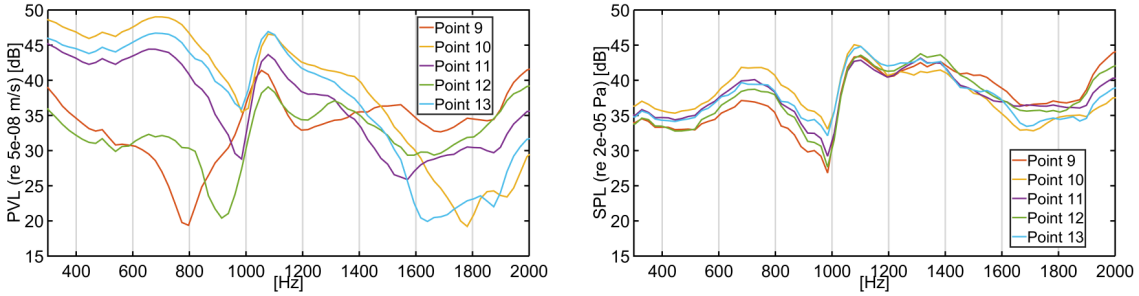

(a) Particle velocity level

(b) Sound pressure level

Figure 7: Spectra of measurement points P9-P13 on the side of the earcup of HP2B

To match the points where the reference microphones are positioned in Figure 1, P9 at the center on the side, P1, P3, and P4 on the ring of the earcup (see Figure 8) are selected, with P9 corresponding to PO, P1 to PB, and the area between P3 and P4 to PA (see PO, PA and PB in Figure 1).

Similar as in Figure 7(a), P9 shows anti-resonance at around 800 Hz in the PVL spectrum (Figure 8(a)). On the contrast, the SPL spectra show no significant difference between the selected four points (Figure 8(b)). Although P3 has higher PVL than P9, it seems that the anti-resonance at P9 is the key factor to make it outperform as in Figure 2. This anti-resonance was not captured by the microphone of the PU probe, but it can be measured by the reference microphone which is on the structure of the earcup. As mentioned in Section 2, apart from the anti-resonance of P9, higher correlation between the reference and error microphones could be another reason to explain the better performance of P9 being the reference microphone position. The leakage can also cause deviations

in the error signal. However, it is also required to investigate the positioning of the error microphone to study the correlation. This is out of the scope of this work and thus will not be further discussed.

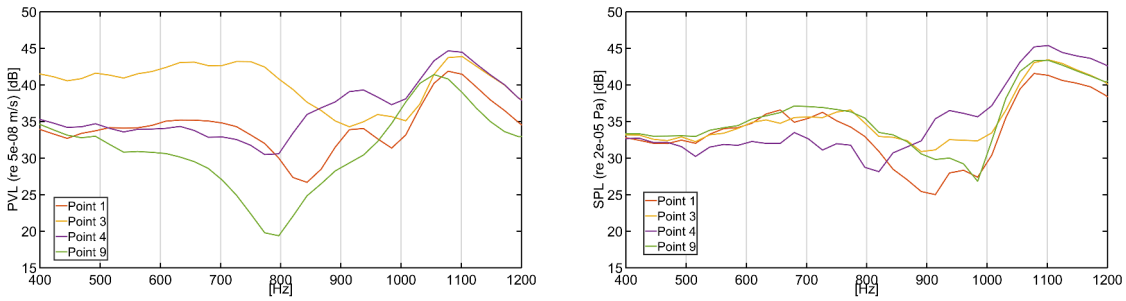

(a) Particle velocity level *(b) Sound pressure level*

Figure 8: Spectra of measurement points P1, P3, P4 and P9 on the ring and the side of the earcup of HP2B

4. 3D SOUND FIELD VISUALIZATION WITH SCAN & PAINT 3D

Although the main leaking spots have already been identified in different frequency ranges with Voyager, it can be very useful to visualize the sound field around the device in order to identify leakages and structural resonances in a more straightforward manner.

The sound visualization system used to capture the information hereby presented is Scan & Paint 3D [14]. The Scan & Paint 3D system uses a 3D sound intensity probe comprising one microphone and three orthogonal particle velocity sensors to capture the full acoustic information of the sound field. The probe is attached to a sphere with IR reflectors, which is tracked by a stereo camera. Thus the scanning trajectories of the probe can be obtained [14, 15]. Figure 9 shows the measurement setup with Scan & Paint 3D.

Figure 9: Measurement setup with Scan & Paint 3D

Multiple measurements were performed around one side of the headphones (same side as in the Voyager measurements), aiming to achieve sound mappings of high spatial resolution. A total of 11

scans adding up to approximately 8 minutes were captured using the Scan & Paint 3D system. All results presented below were obtained after applying a spatial discretization of 3 mm cuboid cells, indicating 3 mm spatial resolution. Figure 10 shows the 3D visualization of the particle velocity field around the HP2B headphone earcup in two perspectives in two frequency ranges, 600 - 1000 Hz and 1000 - 1500 Hz. In both ranges, the bottom of the cushion is the main leakage spot. In 600 - 1000 Hz, the middle and bottom areas of the earcup side show anti-resonance, which is in line with the results measured with Voyager (see Figure 7(a) and Figure 8(a)). Besides, it shows that the top left and right parts of the ring resonate in this frequency range.

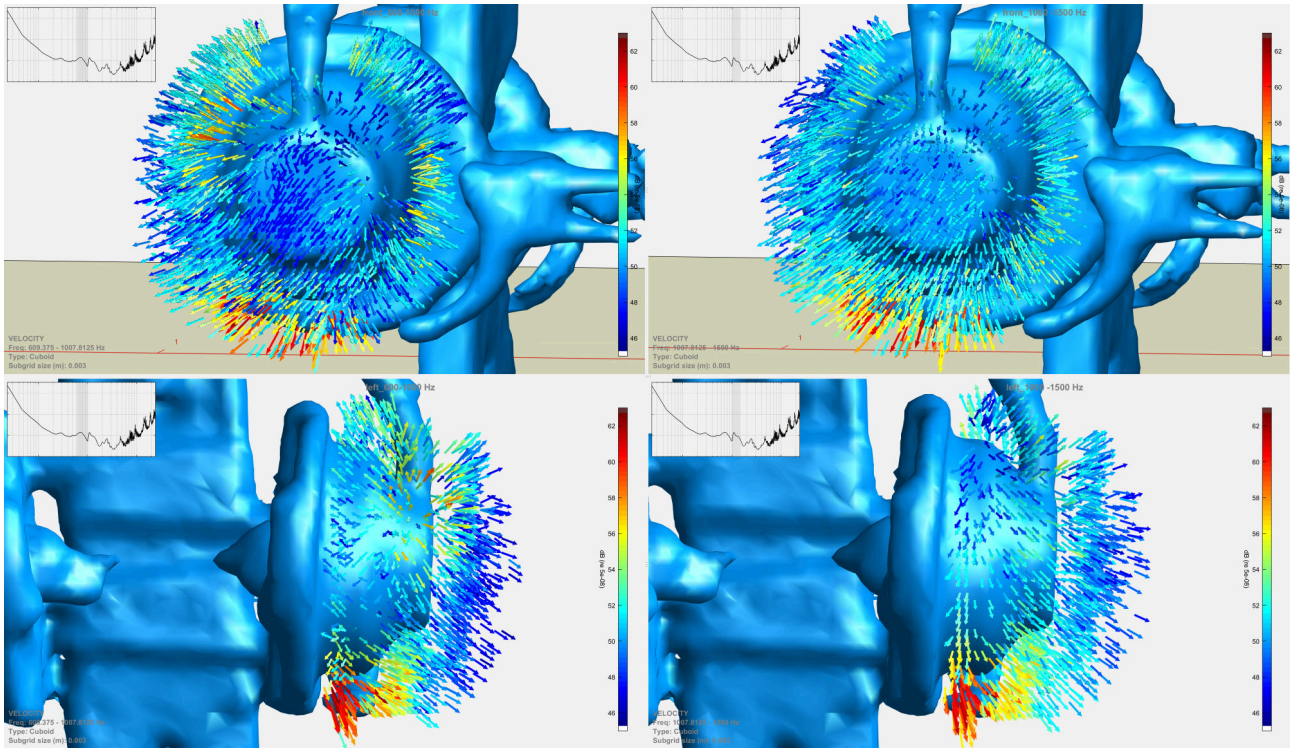

Figure 10: 3D visualization of the particle velocity field around the earcup of HP2B. The first row shows the front view in two frequency ranges, 600 - 1000 Hz (left column) and 1000 - 1500 Hz (right column); the second row shows the side views in the same frequency ranges

The pressure field visualization is illustrated in Figure 11. The bottom of the cushion can be seen as the main leakage spot in 600 - 1000 Hz. Whereas in 1000 - 1500 Hz, the wide distribution of high pressure around the earcup hardened the detection of the leakage. The lack of directivity and surface displacement capture lead to the pressure sensor failing to detect the vibro-acoustic behaviour of the earcup. The 3D visualization facilitates the localization of the main leakage and resonances/anti-resonances over the whole earcup, and shows the advantages of particle velocity.

Despite that ANC focuses on mid-low frequencies, it is still interesting to evaluate the passive sound insulation performance at higher frequencies. Figure 12 shows the sound intensity fields in 2200 - 2600 Hz and 4150 - 5130 Hz. In the left column of Figure 12, two perspectives of the sound intensity field in 2200 - 2600 Hz are shown. The bottom of the cushion remains the main leakage spot. Besides, the resonance on the side of the earcup can be visualized, as well as two nodes on the ring of the earcup (left bottom of Figure 12). In 4150 - 5130 Hz (right column of Figure 12), a leakage spot, top left of the cushion, and two anti-nodes, top left and bottom right of the earcup can be visualized. The middle of the earcup shows anti-resonance pattern. These leakage spots and resonances/anti-resonances have to be taken into consideration to help improve the structure design and material selection. The structure and material, on the other hand, will have acoustic influence at lower frequencies and hence affect the ANC performance. Therefore, it would be recommended to

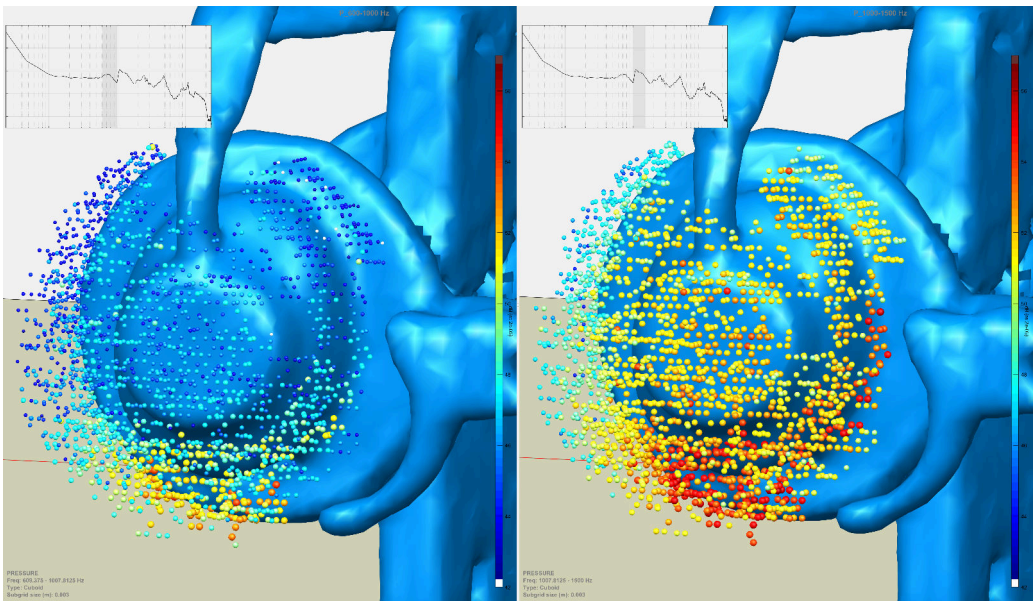

Figure 11: Visualization of the pressure field around the earcup of HP2B. The first row shows the front view in two frequency ranges, 600 - 1000 Hz (left) and 1000 - 1500 Hz (right); the second row shows the side views in the same frequency ranges

combine passive and active noise reduction as a whole, to study and deliver a good performance in a broad frequency range.

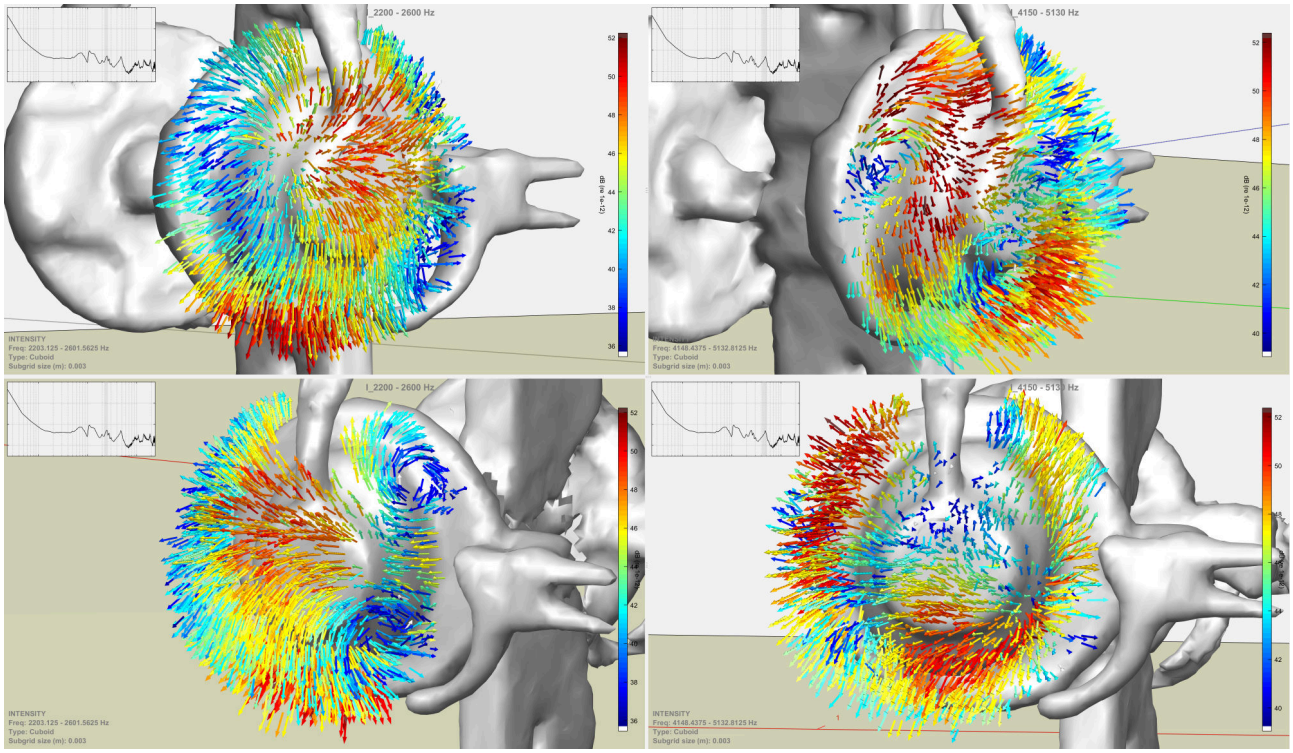

Figure 12: 3D visualization of the sound intensity field around the earcup of HP2B in the frequency range of 2200 Hz - 2600 Hz (left column) and 4150 Hz - 5130 Hz (right column) in two perspectives. Note that it is still HP2B but with a grey colour for the purpose of clear visualization of the intensity vectors

5. CONCLUSIONS

This paper investigated the sound leakage around ANC headphones using particle velocity sensors via fast detection and full 3D sound field visualization. The feedforward ANC performance was deviated when placing the reference microphone on different locations on the headphone earcup. The particle velocity sensor outperforms pressure microphone in detecting the individual differences between different headphones and among several areas on the earcup of the headphone under study, by virtue of its intrinsic higher spatial resolution while measuring in the acoustic near-field. It was discovered that large variations in the sound field can be found around the headphone's mechanical components, with distinctive spectral differences. The inhomogeneous leakage distribution can be the main reason for the different ANC performance with reference microphones on different positions. The bottom of the cushion is the main leakage spot in a broad frequency range for the studied headphone in this work. More importantly, modal behaviour was observed in both the particle velocity spectra and 3D particle velocity field.

Further work on positioning the reference microphone on various locations of the earcup needs to be done to understand how the leakage and resonance influence the ANC performance. In addition, it is necessary to combine the study of positioning the error microphone to explore the correlation of signals measured by the reference and error microphones.

6. ACKNOWLEDGEMENTS

The authors would like to thank Landtop Technologies for performing the Scan & Paint 3D measurements presented in the experimental investigation.

6. REFERENCES

[1] C. Hansen, S. Snyder, X. Qiu, L. Brooks, and D. Moreau, *Active control of noise and vibration*. CRC press, 2012.

[2] Y. Kajikawa, W.-S. Gan, and S. M. Kuo, "Recent advances on active noise control: open issues and innovative applications," *APSIPA Transactions on Signal and Information Processing*, vol. 1, 2012.

[3] S. Liebich, J.-G. Richter, J. Fabry, C. Durand, J. Fels, and P. Jax, "Direction-of-arrival dependency of active noise cancellation headphones," in *ASME 2018 Noise Control and Acoustics Division Session presented at INTERNOISE 2018*, American Society of Mechanical Engineers Digital Collection, 2018.

[4] K. Iwai, S. Kinoshita, and Y. Kajikawa, "Multichannel feedforward active noise control system combined with noise source separation by microphone arrays," *Journal of Sound and Vibration*, vol. 453, pp. 151–173, 2019.

[5] S. M. Kuo, S. Mitra, and W.-S. Gan, "Active noise control system for headphone applications," *IEEE Transactions on Control Systems Technology*, vol. 14, no. 2, pp. 331–335, 2006.

[6] M. Guldenschuh, A. Sontacchi, M. Perkmann, and M. Opitz, "Assessment of active noise cancelling headphones," in *2012 IEEE Second International Conference on Consumer Electronics-Berlin (ICCE-Berlin)*, pp. 299–303, IEEE, 2012.

[7] M. T. Akhtar and W. Mitsuhashi, "Improving performance of hybrid active noise control systems for uncorrelated narrowband disturbances," *IEEE transactions on audio, speech, and language processing*, vol. 19, no. 7, pp. 2058–2066, 2011.

[8] M. Guldenschuh and R. De Callafon, "Detection of secondary-path irregularities in active noise control headphones," *IEEE/ACM transactions on audio, speech, and language processing*, vol. 22, no. 7, pp. 1148–1157, 2014.

[9] L. Wu, X. Qiu, J. Ma, and Y. Guo, "Effects of physical configurations on anc headphone performance," in *24th International Congress on Sound and Vibration, ICSV 2017*, 2017.

[10] O. J. Tobias and R. Seara, "Leaky-fxlms algorithm: stochastic analysis for gaussian data and secondary path modeling error," *IEEE Transactions on speech and audio processing*, vol. 13, no. 6, pp. 1217–1230, 2005.

[11] D. Fernandez Comesana, F. Yang, and E. Tus, "Influence of background noise on non-contact vibration measurements using particle velocity sensors," in *INTER-NOISE and NOISE-CON Congress and Conference Proceedings*, vol. 249, pp. 1871–1876, Institute of Noise Control Engineering, 2014.

[12] D. F. Comesaña, K. Holland, and E. Fernandez-Grande, "Spatial resolution limits for the localization of noise sources using direct sound mapping," *Journal of Sound and Vibration*, vol. 375, pp. 53–62, 2016.

[13] A. Grosso, H.-E. De Bree, S. Steltenpool, and E. Tijs, "Scan and paint for acoustic leakage inside the car," tech. rep., SAE Technical Paper, 2011.

[14] D. F. Comesaña, S. Steltenpool, M. Korbasiewicz, and E. Tijs, "Direct acoustic vector field mapping: new scanning tools for measuring 3d sound intensity in 3d space," in *Proc. Euronoise*, pp. 891–895, 2015.

[15] F. Meng, D. Fernandez Comesana, and S. Steltenpool, "Comparison of 2d and 3d scanning solutions for sound visualization," in *INTER-NOISE and NOISE-CON Congress and Conference Proceedings*, vol. 259, pp. 3926–3937, Institute of Noise Control Engineering, 2019.

[16] https://www.microflown.com/products/portable-measuring-systems/voyager/. Microflown Technologies.

[17] D. F. Comesana and J. Tatlow, "Designing the damping treatment of a vehicle body based on scanning particle velocity measurements,"